PNAS
www.pnas.org

Main Manuscript for

Summertime Stationary Waves Integrate Tropical and Extratropical Impacts on Tropical Cyclone Activity

Zhuo Wang[a]*, Gan Zhang[b], Timothy J. Dunkerton[c] and Fei-Fei Jin[d]

[a]Department of Atmospheric Sciences, University of Illinois at Urbana–Champaign

[b]Atmospheric and Oceanic Sciences Program, Princeton University, and

NOAA/Geophysical Fluid Dynamics Laboratory, Princeton, New Jersey

[c]Northwest Research Associates, Inc., Redmond, Washington, USA

[d]Department of Meteorology, University of Hawaii at Manoa

*Corresponding author: Zhuo Wang, zhuowang@illinois.edu

Classification: Earth, Atmospheric, and Planetary Sciences

Keywords: tropical cyclone variability, tropical upper-tropospheric troughs, stationary waves, Rossby wave breaking, tropical and extratropical interaction, weather-climate connection

Author Contributions: ZW designed the research; ZW and GZ analyzed the data and made the plots; ZW wrote the manuscript; GZ, TD and FJ all participated in discussion and provided feedback on the manuscript.

This PDF file includes:

Main Text, Figures 1 to 4, Table 1

Abstract

Tropical cyclones (TC) are one of the most severe storm systems on Earth and cause significant loss of life and property upon landfall in coastal areas. A better understanding of their variability mechanisms will help improve the TC seasonal prediction skill and mitigate the destructive impacts of the storms. Early studies focused primarily on tropical processes in regulating the variability of TC activity, while recent studies suggested also some long-range impacts of extratropical processes, such as lateral transport of dry air and potential vorticity by large-scale waves. Here we show that stationary waves in the Northern Hemisphere integrate tropical and extratropical impacts on TC activity in July through October. In particular, the tropical upper-tropospheric troughs (TUTTs), as part of the summertime stationary waves, are associated with the variability of large-scale environmental conditions in the tropical North Atlantic and North Pacific and significantly correlated to the variability of TC activity in these basins. TUTTs are subject to the modulation of diabatic heating in various regions and are the preferred locations for extratropical Rossby wave breaking (RWB). A strong TUTT in a basin is associated with enhanced RWB and tropical-extratropical stirring in that basin, and the resultant changes in the tropical atmospheric conditions modulate TC activity. In addition, the anticorrelation of TUTTs between the North Atlantic and North Pacific makes the TC activity indices over the two basins compensate each other, rendering the global TC activity less variable than otherwise would be the case if TUTTs were independent.

Significance Statement

Skillful seasonal prediction of tropical cyclone (TC) activity helps hurricane preparedness and mitigation, especially when the storm impacts are expected to worsen with increasing sea level and water vapor capacity in a warming climate. Slowly varying tropical oceanic conditions have been regarded as a primary source of predictability for TC activity, but recent studies suggested that TC activity is also subject to some long-range impacts of extratropical processes. We show that summertime stationary waves in the Northern Hemisphere, including tropical upper-tropospheric troughs, integrate tropical and extratropical impacts into a unified framework and provide a hemispheric perspective that helps understand the variability and predictability of TC activity over the North Atlantic and North Pacific.

Main Text

1. Introduction

The impacts of tropical cyclones (TC) are expected to worsen with increasing sea level and water vapor capacity in a warming climate. Prior to a hurricane season, the public is concerned whether the upcoming season will be more, or less, active than average. Skillful seasonal prediction of TC activity provides valuable information for storm preparedness and has received increased attention in recent years. While TC prediction has benefitted substantially from advances in numerical models with higher resolution and improved physics parameterizations, a better understanding of the variability mechanisms will also contribute to improved TC prediction.

Tropical cyclone formation, intensification and motion are strongly modulated by tropical atmospheric conditions, including vertical wind shear and tropospheric humidity (1, 2). Although the evolution of individual storms cannot be predicted deterministically beyond the synoptic time scale, TC statistics spanning a longer time scale may be predictable because the large-scale atmospheric circulation in the tropics is closely coupled to slowly varying tropical oceans (3, 4), which are regarded as the primary source of predictability for tropical atmosphere and TC activity (5-9). In addition to coupling to tropical oceans, tropical atmospheric circulation also interacts actively with extratropical atmosphere. On the one hand, the tropics, as the primary terrestrial source of heat, moisture, and angular momentum for the global climate system, modulate extratropical atmospheric circulation via teleconnections and the meridional overturning circulation (10). On the other hand, tropical atmospheric circulation is subject to the impacts of extratropical processes. In a seminal study (11), Charney proposed the view that the large-scale tropical atmospheric circulation is driven by the lateral coupling with precipitating regions and with the extratropics given the weak coupling between vertical motion and horizontal circulation in the tropics. In other words, the extratropics not only respond to but also feed back to the tropics.

Rossby waves represent an important process for extratropical atmospheric circulation to feed back to tropical atmospheric circulation. Extratropical Rossby wavetrains and the attendant Rossby wave breaking (RWB), aided by westerly ducts (12), may penetrate into the tropics and affect tropical convection and change the atmospheric tracer distribution (13-15). In contrast to teleconnections associated with low-frequency climate modes, RWB is a transient, nonlinear process (16). Although RWB occurs on the synoptic time scale, repeated occurrence of RWB enhances the mixing between the tropics and extratropics and can lead to significant anomalies in wind, temperature and humidity fields on the subseasonal and longer time scales and thereby modulate TC activity (17-20). Rossby wave breaking is affected by both tropical and extratropical processes (21-23). Semi-idealized regional numerical experiments demonstrate that the extratropical processes contribute to the interannual variability of Atlantic TC activity and that the impacts can exceed the direct impacts of local SST in some years (24, 25). Overall, these studies suggest that we need to look beyond the tropics to understand the variability of TC activity.

The objective of this study is to provide a unified framework integrating tropical and extratropical impacts on TC activity, highlighting the tropical-extratropical connection. We will invoke the concepts of tropical upper-tropospheric troughs (TUTTs) and summertime stationary waves. TUTTs, also known as mid-ocean troughs (26, 27), are the preferred locations for RWB (28, 29). Characterized by reduced meridional potential vorticity (PV) gradient, TUTTs "break" the barrier of strong PV gradient along the subtropical jet that hinders geostrophic mixing (Fig. S1) and can be regarded as "windows" for active tropical-extratropical interaction (12, 30). Along with the upper-level monsoon anticyclones, TUTTs constitute the summertime subtropical stationary waves (31, 32). The variability of TUTTs can be understood in the context of stationary waves, which are planetary waves modulated by global diabatic heating, topographic effect, and transient eddy feedback (31, 32). We will show that summertime stationary waves integrate tropical and extratropical impacts and provide a hemispheric perspective on the variability of TC activity over the North Atlantic and North Pacific basins.

2. Results

2.1 TUTTs and the large-scale circulation anomalies modulating TC activity

TUTTs are characterized by a cold-core, shallow structure in the upper troposphere (27). They are present over the North Pacific and North Atlantic in boreal summer and extend equatorward and westward from the subtropics to the tropics (Fig. S1). To quantify the relationship between TUTTs and TC activity, a TUTT index is defined based on the equatorward extension of the upper-level westerly flow over a subtropical ocean (see the definition of a TUTT index in "Data and Methods"). We focus on the bulk of TC season over the North Atlantic and North Pacific, July-October (JASO), during 1979-2018. Two TUTT indices are derived, one representing the North Pacific TUTT (TUTT_Pac) and the other the North Atlantic TUTT (TUTT_Atl) (Fig. S2a). TUTT_Pac extends from the subtropical East Pacific to the tropical Central Pacific, while TUTT_Atl has a smaller latitude range but spans the entire Atlantic in the east-west direction, including the Caribbean Sea in most years. It is worth noting that the tropical Central Pacific, where TUTT_Pac resides, is relatively devoid of climatological TC activity, with most TCs to its west or east, whereas the Atlantic has considerable activity that is highly variable both in regard to the basin-wide storm frequency and regional distribution.

We will first explore the link between TUTTs and the large-scale atmospheric circulation anomalies that modulate TC activity. Composite differences are constructed between strong and weak TUTT years in the respective basins (see composite years in Table S1). As shown in Figs. 1a and 1b, strong TUTT_Atl years are characterized by enhanced vertical wind shear (VWS, defined as the magnitude of the vector wind difference between 200 and 850 hPa) and reduced column water vapor (CWV) in the tropical/subtropical Atlantic, including a major portion of the main development region (MDR; defined here as 10º–25ºN, 20º–80ºW). Since TUTT_Atl is defined based on the zonal wind, a strong link between the TUTT index and VWS is expected, consistent with enhanced upper-level westerlies for a deepened TUTT. Additionally, strong CWV composite anomalies suggest that the TUTT index also relates to the thermodynamics of atmospheric circulation. Furthermore, a strong TUTT is associated with a stronger subtropical high in the lower troposphere and higher sea level pressure over the tropical/subtropical Atlantic (33).

It is worth noting that the composites of VWS and CWV based on TUTT_Atl resemble closely the corresponding composites based on an RWB index that represents the seasonal frequency of RWB over the North Atlantic (Fig. 8 in ref. 18). The similarities can be explained by the strong correlation between the RWB and TUTT_Atl indices ($r=0.80$). RWB frequency increases significantly in strong TUTT years (Fig. 1c), especially over the western Atlantic, which transports cold and dry extratropical air equatorward and increases the thickness gradient and tropospheric dryness to its south (17-19). The extensive upper-level westerlies associated with a deepened TUTT facilitate equatorward Rossby wave propagation (12) and breaking. Meanwhile, transient eddy feedback likely helps maintain or amplify a TUTT (28, 30). The seasonal variability of TUTTs thus reflects the cumulative impacts of RWB beyond the synoptic time scale.

Large-scale circulation anomalies are also found associated with TUTT_Pac (Figs. 1d-f). During strong TUTT_Pac years, CWV is reduced over the central and eastern tropical Pacific and enhanced in the western Pacific; VWS increases in the central and eastern tropical Pacific and decreases in the western tropical Pacific. Similar to TUTT_Atl, TUTT_Pac is related to the variability of RWB, and RWB occurs more frequently over the Central Pacific during strong TUTT_Pac years. However, we caution that the large-scale circulation anomalies associated with TUTTs should not be entirely attributed to RWB. As shown in section 2.3, other factors also modulate TUTTs in addition to the transient eddy feedback related to RWB.

2.2 TUTTs and Tropical Cyclone Activity

Previous studies have shown that upper-level troughs or TUTT cells may facilitate the development of a TC and affect the TC track at the synoptic time scale (34, 35). Here we will focus on the seasonal time scale. Given the circulation anomalies (Fig. 1), it is not a surprise to see a strong link between the seasonal TC activity and TUTTs. As shown in Fig. 2a, strong Atlantic TUTT years are characterized by a basin-wide reduction of track density function (TDF) in the North Atlantic, consistent with reduced CWV and enhanced VWS over the Atlantic MDR (33). Significant negative correlations are found between TUTT_Atl and the basin-wide TC frequency (TCF), hurricane frequency (HURR) and accumulative cyclone energy (ACE) (Table 1). In fact, the seasonal correlations of the Atlantic TC indices with TUTT_Atl are much stronger than the corresponding correlations with the Nino3.4 or the Atlantic MDR SST index (Table 1).

Over the eastern Pacific, reduced CWV and enhanced VWS in strong TUTT_Pac years (Figs. 1d-f) lead to a decrease in TC activity except in a small region south of the Gulf of California (Fig. 2b), where enhanced TC activity may be related to Central American gap winds (36). Over the western Pacific, the changes of CWV and VWS have a more complicated spatial pattern (Figs. 1d-f). East of 150ºE, negative CWV anomalies and positive VWS anomalies are dominant between 10º–25ºN, the main latitude band for TC genesis, while positive CWV anomalies and negative VWS anomalies largely occur poleward or equatorward of this latitude band. West of 150ºE, enhanced CWV occurs off the coast along with weak VWS anomalies. As a consequence, tropical cyclogenesis frequency decreases east of 150ºE and does not change much west of 150ºE (Fig. S3), corresponding to a westward shift (37) in addition to a basin-wide reduction. The reduced genesis frequency east of 150ºE contributes to decreased TDF both locally and downstream. Negative TDF anomalies thus prevail over the western Pacific except in the East China Sea region, where the environmental conditions are favorable. The pattern bears a resemblance to the TC activity anomalies related to the El Niño-Southern Oscillation (ENSO) reported in previous studies (38, 39), but the significant negative correlations between TC indices and TUTT_Pac over the western and eastern Pacific are stronger than the corresponding correlations with an ENSO index, some of which are insignificant or even close to zero (Table 1; also see 40).

Another interesting feature in the TDF composites is the out-of-phase TC variability between the Atlantic and Pacific basins, which is consistent with the seesaw tendency of the Pacific and Atlantic TUTTs (Fig. S2b). The anticorrelation between TUTT_Pac and TUTT_Atl ($r=-0.59$) can be explained by the PV impermeability theorem (41). If the atmosphere is in a quasi-steady state and the PV fluxes associated with diabatic heating and friction are negligible, the PV impermeability theorem requires that the poleward advective PV flux closely balance the equatorward advective PV flux (42, 43). The poleward advective PV flux is mainly determined by the zonal mean meridional overturning circulation, while the equatorward advective PV flux occurs primarily in the TUTT regions during summer (41). The variability of equatorward PV fluxes over the two basins tends to compensate each other unless there is a substantial change in the poleward advective PV flux. An important implication is the out-of-phase relationship of TC activities between the Atlantic and Pacific basins [r=-0.47, -0.44 and -0.42 for TCF, HURR and ACE between the North Pacific (the sum of the western and eastern Pacific) and North Atlantic, respectively]. Since the North Pacific and North Atlantic together account for more than 60% of the global TC frequency, the anticorrelation between the two basins makes the global TC activity less variable (44, 45). This TC anticorrelation between the North Pacific and North Atlantic has been examined in some previous studies and attributed to the modulation by the Walker circulation or changes in tropospheric static stability related to relative SST (46-49). TUTTs offer an additional mechanism for this inter-basin relationship. Further analysis shows that the anticorrelation between TUTT_Atl and TUTT_Pac is much weaker on the monthly time scale, possibly because the quasi-steady state assumption breaks down on the shorter time scales.

2.3 Summertime Stationary waves

Given the strong link between TUTTs and TCs, one may ponder what drives the variability of TUTTs. Recalling that TUTTs are part of the summertime stationary waves, we carried out an empirical orthogonal function (EOF) analysis to extract the dominant mode of variability of 200-hPa streamfunction field between 15°S-75°N. To focus on stationary waves, the zonal mean was removed and the data were detrended prior to the EOF analysis. The leading EOF mode (EOF1) explains 46% of the total variance and is well separated from the remaining modes (Fig. S4). It consists of a wavenumber-one pattern in the tropics/subtropics and higher wavenumber patterns in the extratropics (Fig. 3a). The former is associated with the variability of the Walker circulation, reminiscent of the impacts of the ENSO (Fig. S5). In the extratropics, of particular interest to this study is a wavetrain pattern emanating from the Central Pacific. It spans across the North Pacific and North America and extends to the subtropical North Atlantic, following a great-circle route. The wavetrain contributes to an out-of-phase relation between the subtropical Central Pacific and the subtropical Atlantic, and it resembles the wavetrain that modulates RWB occurrence over the West Atlantic (Fig. 1d in ref. 23). The time series of EOF1 is significantly correlated with TUTT_Pac ($r=0.72$) and TUTT_Atl ($r=-0.82$) (Fig. 3b) and also strongly correlated to the HURR and ACE indices in the three basins (Table 1).

EOF1 is characterized by a baroclinic vertical structure in the tropics/subtropics and a barotropic structure in the extratropics (Fig. S6). The different vertical structures are consistent with previous studies and indicate the role of diabatic heating in maintaining the stationary waves in the tropics/subtropics and the importance of Rossby wave energy dispersion, topographic effect, and transient eddy feedback in the extratropics (32, 50). To investigate the forcing mechanisms of EOF1, correlations are calculated between the time series of EOF1 and SST/precipitation at each grid point.

A horseshoe pattern of SST signals (Fig. 4a) is present over the Pacific, with significant positive correlations over the Central and East Pacific and negative correlations extending from the equatorial West Pacific poleward in both hemispheres. The pattern has stronger signals in the extratropical Pacific than the ENSO pattern (Fig. S5), and resembles the Pacific Decadal Oscillation (PDO). Meanwhile, negative correlations prevail over the tropical and extratropical North Atlantic and are reminiscent of the Atlantic tripolar SST pattern. EOF1 is found significantly correlated to the ENSO and PDO indices (Table S2). Additionally, the positive phase of EOF1 is associated with reduced precipitation over the tropical Central and East Pacific and enhanced precipitation over the Indian summer monsoon region, the Maritime Content, Australia, Central America, the tropical/subtropical Atlantic, and the African monsoon region (Fig. 4b).

Although the SST and precipitation correlation maps strongly resemble the impacts of the ENSO (Fig. S5), we stress that the variability of the summertime stationary waves or TUTTs cannot be completely attributed to the ENSO, which is much weaker in summer than in winter. To better illustrate this point, the linear impacts of the ENSO are removed from the time series of EOF1 and the field variables of interest using the linear least squares regression on the Nino3.4 index, and correlation maps are constructed with the residual signals (right panels in Fig. 4). After the removal of the ENSO, the SST signals are weakened in the tropical Pacific but remain largely unchanged in the extratropical Pacific and are slightly enhanced in the North Atlantic; significant correlations with precipitation remain over the subtropical Pacific, the Maritime Continent, the Indian summer monsoon region, Central America and the tropical Atlantic; and the partial correlation map between EOF1 and H200 has weaker signals over the tropical Pacific, but the signals in the northern extratropics, including the wavetrain spanning from the Central Pacific to the subtropical North Atlantic, remain significant or are even slightly enhanced (Figs. 4c and 4f). These results are consistent with previous findings that the diabatic heating over various monsoon regions helps maintain stationary waves (32, 50). In particular, it was suggested that a monsoon anticyclone and the TUTT to its east are associated with an east-west overturning circulation, and the dryness in the descending branch over the ocean helps maintain the TUTT via radiative cooling (51, 33). Since the subtropical stationary waves have a first-baroclinic mode structure (31, 32), the enhanced shear is a byproduct of a stronger upper-level trough sitting over a stronger low-level subtropical high. Over the Pacific, a strong TUTT is also accompanied by a weakened monsoon trough over the western Pacific (Fig. S7). These conditions all contribute to suppressed TC activity in strong TUTT years. The large spatial scale of stationary waves highlights the global nature of TC variability.

The correlations between TUTT indices and various climate indices are examined as well. Each TUTT index is significantly correlated to several climate indices, including the Nino3.4, PDO, the Atlantic meridional mode (AMM, 7), the Atlantic Multidecadal Oscillation (AMO), and the Atlantic MDR SST (Table S2) (52, 53, 33). The PDO and TUTT_Pac, and the AMO and TUTT_Atl, may be linked via RWB in the respective basins (54, 55). Although the ENSO contributes to the anticorrelation between TUTT_Pac and TUTT_Atl, the partial correlation between TUTT_Pac and TUTT_Atl remains significant ($r=-0.39$) after the influence of the ENSO is removed using linear regression. Additionally, the negative correlation between the TUTT and ACE indices of the same basin remains significant after the removal of the linear impacts of the ENSO (Fig. S8).

We stress that TUTTs (or stationary waves) not only reflect the contribution from the slowly varying tropical SST but also extratropical impacts. The latter is supported by the strong statistical link between TUTT indices and RWB (Fig. 1). To further demonstrate this point, the Atlantic ACE index is reconstructed using a linear regression model with various indices. The MDR SST alone explains 30.3% of the ACE variance during 1979-2018; the MDR SST and the tropical mean SST (averaged between 30ºS-30ºN) together explain 39.7% of the variance; and the explained variance increases to 62.4% by adding TUTT_Atl (Fig. S9). This suggests that skillful prediction of stationary waves and TUTTs will help improve TC seasonal prediction.

2.4 A statistical assessment of TUTT predictability

Given the abovementioned statistical linkages, we attempt to predict the EOF1 and TUTT indices in JASO using SST indices during April-June. We tested different pairs of possible predictors among the AMO, PDO, Nino3.4 and the Atlantic MDR SST, and constructed multiple linear regression (MLR) models. The AMO and Nino3.4 are the best pair to predict TUTT_Atl and EOF1, and the PDO and Atlantic MDR SST are the best pair to predict TUTT_Pac (Fig. S10), suggesting that a TUTT is modulated by SST in both the local basin and a remote basin. The anomaly correlation coefficients between the predicted and observed time series using the leave-five-out method (see data and methods) are 0.72, 0.53 and 0.57 for TUTT_Atl, TUTT_Pac and EOF1, respectively. The prediction skill using this simple statistical model represents the lower bound of the seasonal predictability of summertime stationary waves and TUTTs with the caveat that the sample size is not very large and cross validation may overestimate the prediction skill (56). Although the predictors have information on tropical SST, we caution that the AMO and PDO both include extratropical information, and that the physical processes linking tropical SST and TUTTs (or stationary waves) may not be purely tropical as implied by the recent semi-idealized numerical model studies (24, 25). A better understanding of the TUTT variability that is unrelated to tropical SST will help better understand the predictability of TC activity and merits further study.

3. Summary and Discussion

We demonstrated the strong link between TUTTs and TC activity over the North Pacific and North Atlantic. As part of the summertime stationary waves, TUTTs are related to tropical and extratropical SST and precipitation anomalies in various regions, including the ENSO and monsoons. Additionally, TUTTs are the preferred regions for RWB, and reflect the cumulative effects of RWB beyond the synoptic scale. Active RWB in a strong TUTT year contributes to enhanced vertical wind shear and reduced tropospheric humidity, and may help amplify the TUTT via the transient eddy feedback. Radiative forcing associated with the changes in the humidity field may play a role in maintaining TUTTs as well (33). Our analysis suggests that stationary waves integrate tropical and extratropical impacts on TC activity and provide a hemispheric perspective on the variability of TC activity over the North Pacific and North Atlantic. In addition, the Atlantic TUTT and the Pacific TUTT tend to vary out of phase due to the PV impermeability nature, and the seesaw relationship of the Pacific and Atlantic TUTTs contributes to an anticorrelation of TC activity between the two basins, which makes the global TC activity less variable. Finally, because TUTTs are connected to monsoons and extratropical Rossby waves, they introduce a factor other than tropical SST for the variability of TC activity. Overall, this study advocates a hemispheric perspective that helps understand the variability and predictability of TC activity over the North Atlantic and North Pacific. This view may also help understand the projection of TC activity in future climate.

4. Materials and Methods

The JASO seasonal mean data on isobaric surfaces from the ERA-Interim reanalysis are used to examine the atmospheric circulation anomalies, and the 6-hourly PV field on the 350-K isentropic surface is used to detect anticyclonic RWB (57, 17). RWB frequency is in units of percent and is defined as the frequency of high-PV tongue centroids associated with RWB in a $5^{\circ} \times 5^{\circ}$ resolution grid mesh, smoothed with four-point averaging. Additionally, we use precipitation data from the Global Precipitation Climatology Project, SST from the Extended Reconstructed Sea Surface Temperature Version 5, and TC track and intensity data from the IBTrACS. The Nino3.4

SST index is used to represent the ENSO, and along with the other indices, is downloaded from the NOAA Physical Science Laboratory.

To quantitatively evaluate the variability of the TUTTs and their links to TCs and RWB, a TUTT index is defined using the 200-hPa geopotential height (H200) field. First, the geostrophic zonal wind is derived from H200 with a fixed Coriolis parameter (*f*) at 15ºN (denoted as u_g). The zonal mean latitude of the circumglobal contour of the long-term seasonal mean $u_g = 1.0\ m\ s^{-1}$, which turns out to be just south of 20ºN, is chosen as a reference latitude, and the area where the circumglobal contour of the seasonal mean $u_g = 1.0\ m\ s^{-1}$ extends equatorward of the reference latitude is defined as the TUTT index of an oceanic basin. We chose to use the constant-*f* geostrophic zonal wind rather than the total zonal wind because the weak westerly flow in the latter field occasionally extends across the equator and connects to westerlies in the Southern hemisphere. The choice of a small positive value $1.0\ m\ s^{-1}$, instead of zero, helps increase the robustness of the results, and varying this value from 0.5 to $1.5\ m\ s^{-1}$ does not qualitatively change our results. Varying the Coriolis parameter in the calculation of u_g is equivalent to choosing a different contour threshold for u_g. A TUTT index defined this way focuses on the westerly flow in the eastern half of a TUTT and mainly describes the extent of a TUTT, although one can define the intensity and the longitudinal and latitudinal locations of a TUTT as well.

The leave-five-out method is used to assess the skill of an MLR model. For a time series of n observations, we leave five consecutive observations out as a test dataset (e.g., 1, 2, .., 5) and develop an MLR based on the remaining n-5 observations (e.g., 5, 6, …, n). The model is then used to predict the five test data points. This procedure is repeated for different test datasets (1-5, 6-10, etc.) to predict all observations, yielding a time series of the predicted variable. The correlation between the predicted and observed time series is calculated to assess the prediction skill. The leave-five-out cross validation is chosen over leave-one-out to take care of the biennial tendency of the large-scale atmospheric variability.

Data Availability

The IBTrACS data are available at https://www. ncdc.noaa.gov/ibtracs/. The climate indices are available from the NOAA Physical Science Laboratory (https://www.psl.noaa.gov/data/). The normalized TUTT indices are available in Dataset S1. The ERA-Interim reanalysis data are downloaded from the National Center for Atmospheric Research (NCAR) Research Data Archive (https://rda.ucar.edu/datasets/ds627.0/). The GPCP precipitation data are available at https://psl.noaa.gov/data/gridded/data.gpcp.html. The ERSST data are available at https://www.ncdc.noaa.gov/data-access/marineocean-data/extended-reconstructed-sea-surface-temperature-ersst-v5.

Acknowledgements

This work is supported by the National Oceanic and Atmospheric Administration (NOAA) Grant NA16OAR4310080 and NA18OAR4310271.

References

1. W.-M. Gray, Global view of the origin of tropical disturbances and storms. *Mon. Wea. Rev.*, **96**, 669–700 (1968).
2. Tang, B. and coauthors, Recent advances in research on tropical cyclogenesis. *Tropical Cyclone Research and Review*, in press (2020).
3. J.-D. Neelin, and I. M. Held, Modeling tropical convergence based on the moist static energy budget. *Mon. Wea. Rev.*, **115**, 3–12 (1987).
4. R.-S. Lindzen, and S. Nigam, On the role of sea surface temperature gradients in forcing low-level winds and convergence in the Tropics. *J. Atmos. Sci.,* **44**, 2418–2436 (1987).
5. T.-N. Palmer, "Predictability of the atmosphere and oceans: From days to decades" in Decadal Climate Variability: Dynamics and Predictability, D. L. T. Anderson and J. Willebrand, Eds. (Springer, 1996), pp. 83–151.
6. G.-A. Vecchi, and Coauthors, On the seasonal forecasting of regional tropical cyclone activity. *J. Climate,* **27**, 7994–8016 (2014).
7. J. P. Kossin, and D. J. Vimont, A more general framework for understanding Atlantic hurricane variability and trends. *Bull. Amer. Meteor. Soc.*, **88**, 1767-1781 (2007).
8. S.J. Camargo, A.H. Sobel, A.G. Barnston, and P.J. Klotzbach, The influence of natural climate variability, and seasonal forecasts of tropical cyclone activity, Chapter 11, pp. 325-360, in Global Perspectives on Tropical Cyclones, from Science to Mitigation, 2nd edition, World Scientific Series on Earth System Science in Asia, vol. 4, J.C.L. Chan and J.D. Kepert, editors, ISBN 978-981-4293-47-1 (2010).
9. G. D. Bell, and M. Chelliah, Leading tropical modes associated with interannual and multi-decadal fluctuations in North Atlantic hurricane activity. *J. Climate*, **19**, 590-612 (2006).
10. K.-E. Trenberth, G. W. Branstator, D. Karoly, A. Kumar, N.-C. Lau, and C. Ropelewski, Progress during TOGA in understanding and modeling global teleconnections associated with tropical sea surface temperatures. *J. Geophys. Res.,* **103**(C7), 14291–14324 (1998).
11. J.-G. Charney, A note on large-scale motions in the tropics. *J. Atmos. Sci.*, **20**, 607–609 (1963).
12. P.-J. Webster, and J. R. Holton, Cross-equatorial response to middle- latitude forcing in a zonally varying basic state. *J. Atmos. Sci.,* **39**, 722–733 (1982).
13. G.-N. Kiladis, and K. M. Weickmann, Circulation Anomalies Associated with Tropical Convection during Northern Winter. *Mon. Wea. Rev.,* **120**, 1900–1923 (1992).
14. D.-W. Waugh, and B.M. Funatsu, Intrusions into the Tropical Upper Troposphere: Three-Dimensional Structure and Accompanying Ozone and OLR Distributions. *J. Atmos. Sci.,* **60**, 637–653 (2003).
15. R.-K. Scott, J. P. Cammas, P. Mascart, and C. Stolle, Stratospheric filamentation into the upper tropical troposphere, *J. Geophys. Res.,* **106**, 11835 – 11848 (2001).
16. M.-E. McIntyre, and T. N. Palmer, Breaking planetary waves in the stratosphere. *Nature*, **305**, 593–600 (1983).
17. G. Zhang, Z. Wang, T. Dunkerton, M. Peng, and G. Magnusdottir, Extratropical Impacts on Atlantic Tropical Cyclone Activity, *J. Atmos. Sci.,* **73**, 1401–1418 (2016).
18. G. Zhang, Z. Wang, M. Peng, and G. Magnusdottir, Characteristics and Impacts of Extratropical Rossby Wave Breaking during the Atlantic Hurricane Season, *J. Climate*, **30**, 2363-2379 (2017).

19. P.-P. Papin, Variations in Potential Vorticity Streamer Activity: Development Pathways, Environmental Impacts, and Links to Tropical Cyclone Activity in the North Atlantic Basin. Ph.D. dissertation, The State University of New York at Albany, 226 pp (2017).
20. W. Li, Z. Wang, G. Zhang, M.S. Peng, S.G. Benjamin, and M. Zhao, Subseasonal Variability of Rossby Wave Breaking and Impacts on Tropical Cyclones during the North Atlantic Warm Season. *J. Climate*, **31**, 9679–9695 (2018).
21. G. Rivière, Effect of Latitudinal Variations in Low-Level Baroclinicity on Eddy Life Cycles and Upper-Tropospheric Wave-Breaking Processes. J. Atmos. Sci., 66, 1569–1592 (2009).
22. M. Drouard, G. Rivière, and P. Arbogast, The Link between the North Pacific Climate Variability and the North Atlantic Oscillation via Downstream Propagation of Synoptic Waves. J. Climate, 28, 3957–3976 (2015).
23. G. Zhang, and Z. Wang, North Atlantic Rossby Wave Breaking during the Hurricane Season: Association with Tropical and Extratropical Variability. J. Climate, 32, 3777–3801 (2019).
24. G. Zhang, T. Knutson, and S. Garner, Impacts of Extratropical Weather Perturbations on Tropical Cyclone Activity: Idealized Sensitivity Experiments with a Regional Atmospheric Model. *Geophys. Res. Lett.,* in revision (2019).
25. C.-C. Chang, and Z. Wang, Relative impacts of local and remote forcing on tropical cyclone frequency in numerical model simulations. *Geophys. Res. Lett.,* **45**, 7843–7850 (2018).
26. T.-N. Krishnamurti, Observational study of the tropical upper- tropospheric motion field during the northern hemisphere summer. *J. Appl. Meteor.*, **10**, 1066-1096 (1971).
27. J.-C. Sadler, A role of the tropical upper tropospheric trough in early season typhoon development. *Mon. Wea. Rev.*, **104**, 1266–1278 (1976).
28. G.-A. Postel, and M. H. Hitchman, A Climatology of Rossby Wave Breaking along the Subtropical Tropopause. *J. Atmos. Sci.*, **56**, 359–373 (1999).
29. D.-W. Waugh, and L. M. Polvani, Climatology of Intrusions into the tropical upper troposphere, *Geophys. Res. Lett.,* **27**, 3857–3860 (2000).
30. T. Horinouchi, F. Sassi, and B. Boville, Synoptic-scale Rossby waves and geographic distribution of lateral transport routes between the tropics and the extratropics in the lower stratosphere, *J. Geophys. Res.,* **105**, 26579–26592 (2000).
31. G.-H. White, An observational study of the Northern Hemisphere extratropical summertime general circulation. *J. Atmos. Sci.,* **39**, 24-53 (1982).
32. M. Ting, Maintenance of Northern Summer Stationary Waves in a GCM. *J. Atmos. Sci.,* **51**, 3286–3308 (1994).
33. J.A. Knaff, Implications of Summertime Sea Level Pressure Anomalies in the Tropical Atlantic Region. *J. Climate*, **10**, 789-804, (1997).
34. J. Molinari, and D. Vollaro, External influences on hurricane intensity. Part 1: Outflow layer eddy angular momentum fluxes, *J. Atmos. Sci.*, **46**, 1093–1110 (1989).
35. J.-E. Patla, D. Stevens, and G. M. Barnes, A conceptual model for the influence of TUTT cells on tropical cyclone motion in the northwest Pacific Ocean. *Wea. Forecasting,* **24**, 1215–1235 (2009).
36. D. Fu, P. Chang, and C. M. Patricola, Intrabasin Variability of East Pacific Tropical Cyclones During ENSO Regulated by Central American Gap Winds. *Sci Rep*, **7**, 1658 (2017).
37. L. Wu, C. Wang, and B. Wang, Westward shift of western North Pacific tropical cyclogenesis. *Geophys. Res. Lett.*, **42**, 1537–1542 (2015).

38. H.H. Chia, and C. F. Ropelewski, The interannual variability in the genesis location of tropical cyclones in the northwest Pacific. *J. Climate*, **15**, 2934-2944 (2002).
39. S. J. Camargo, A. W. Robertson, S. J. Gaffney, P. Smyth, and M. Ghil, Cluster analysis of typhoon tracks: Part II: Large-scale circulation and ENSO. *J. Climate*, **20**, 3654-3676 (2007).
40. S. J. Camargo, and A. H. Sobel, Western North Pacific tropical cyclone intensity and ENSO. *J. Climate*, **18**, 2996-3006 (2005).
41. S. Ortega, P. J. Webster, V. Toma, and H. R. Chang, The effect of potential vorticity fluxes on the circulation of the tropical upper troposphere, *Q. J. Roy. Meteor. Soc.*, **144**, 848–860 (2018).
42. P.-H. Haynes, and M. E. McIntyre, On the evolution of vorticity and potential vorticity in the presence of diabatic heating and frictional or other forces. *J. Atmos. Sci.*, **44**, 828–841 (1987).
43. P.-H. Haynes, and M. E. McIntyre, On the conservation and impermeability theorems for potential vorticity. *J. Atmos. Sci.*, **47**, 2021–2031 (1990).
44. M.-A. Lander, and C. P. Guard, A look at global tropical cyclone activity during 1995: Contrasting high Atlantic activity with low activity in other basins. *Mon. Wea. Rev.*, **126**, 1163–1173 (1998).
45. B. Wang, Y. Yang, Q. H. Ding, H. Murakami, and F. Huang, Climate control of the global tropical storm days (1965–2008). *Geophys. Res. Lett.,* **37**, L07704 (2010).
46. K.-L. Swanson, Nonlocality of Atlantic tropical cyclone intensities, *Geochem. Geophys. Geosyst.,* **9**, Q04V01 (2008).
47. C. Wang, and S.-K. Lee, Co-variability of tropical cyclones in the North Atlantic and the eastern North Pacific, *Geophys. Res. Lett.*, **36**, L24702 (2009).
48. G. Zhang, and Z. Wang, Interannual variability of tropical cyclone activity and regional Hadley circulation over the Northeastern Pacific, *Geophys. Res. Lett.,* **42**, 2483-2481 (2015).
49. C.M. Patricola, R. Saravanan, and P. Chang, A teleconnection between Atlantic sea surface temperature and eastern and central North Pacific tropical cyclones. *Geophys. Res. Lett.,* **44**, 1167-1174 (2017).
50. S. Nigam, and E. DeWeaver, Stationary waves (orographic and thermally forced). *Elsevier Science* (2015), pp.431-445
51. V. Magaña, and M. Yanai, Tropical-Midlatitude Interaction on the Time Scale of 30 to 60 Days during the Northern Summer of 1979. *J. Climate*, **4**, 180–201 (1991).
52. Wang, C., and L. Wu, Interannual shift of the tropical upper- tropospheric trough and its influence on tropical cyclone formation over the western North Pacific. *J. Climate*, **29**, 4203–4211 (2016).
53. M. Lu, K. Deng, S. Yang, G. Zhou, and Y. Tan, Interannual and interdecadal variations of the mid-Atlantic trough and associated American–Atlantic–Eurasian climate. *Atmosphere-Ocean*, **55**, 284–292 (2017).
54. C. Strong, and G. Magnusdottir, The Role of Tropospheric Rossby Wave Breaking in the Pacific Decadal Oscillation. *J. Climate*, **22**, 1819–1833 (2009)
55. P. Davini, J. von Hardenberg, and S. Corti, Tropical origin for the impacts of the Atlantic Multidecadal Variability on the Euro-Atlantic climate. *Environ. Res. Lett.* **10**, 094010 (2015).
56. P. W. Mielke, K. J. Berry, C. W. Landsea, and W. M. Gray, Artificial Skill and Validation in Meteorological Forecasting. *Wea. Forecasting*, **11**, 153–169 (1996).
57. C. Strong, and G. Magnusdottir, Tropospheric Rossby wave breaking and the NAO/NAM. *J. Atmos. Sci.*, **65**, 2861–2876 (2008).

Figures and Tables

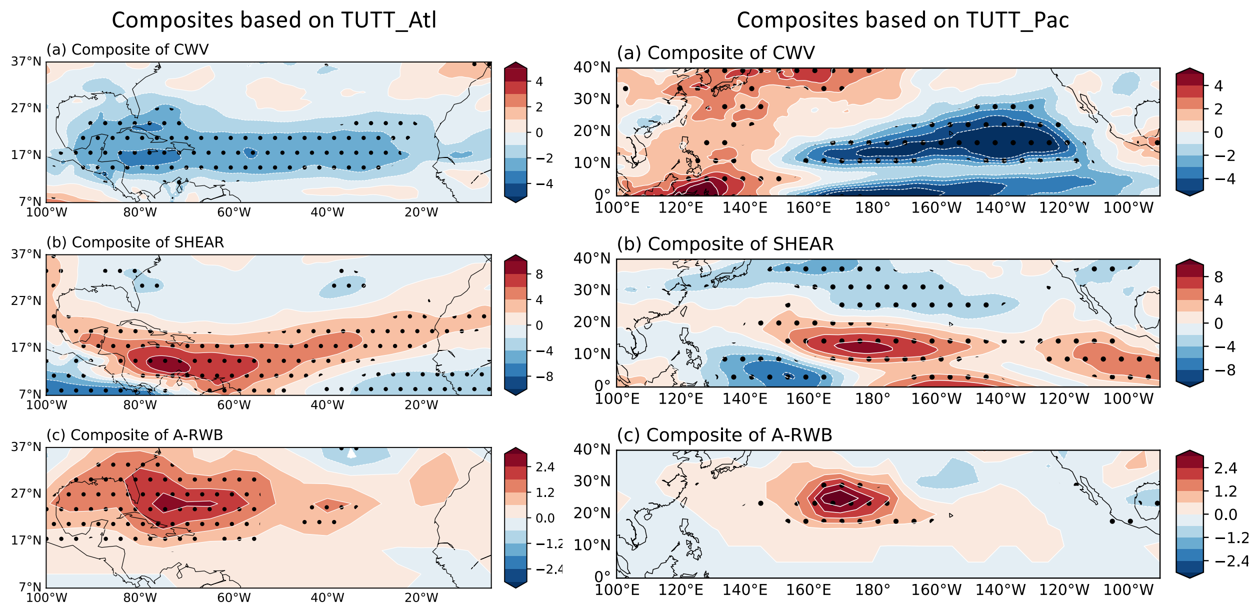

Figure 1 Composite anomalies of (a, d) column water vapor (mm), (b, e) vertical wind shear (m s^{-1}), and (c, f) anticyclonic RWB frequency (%) for the Atlantic basin based on the TUTT_Atl index (left) and for the Pacific basin based on the TUTT_Pac index (right). Black dots highlight the anomalies exceeding the 95% confidence level. Note that the latitude-longitude ranges of the plots are different for the two basins.

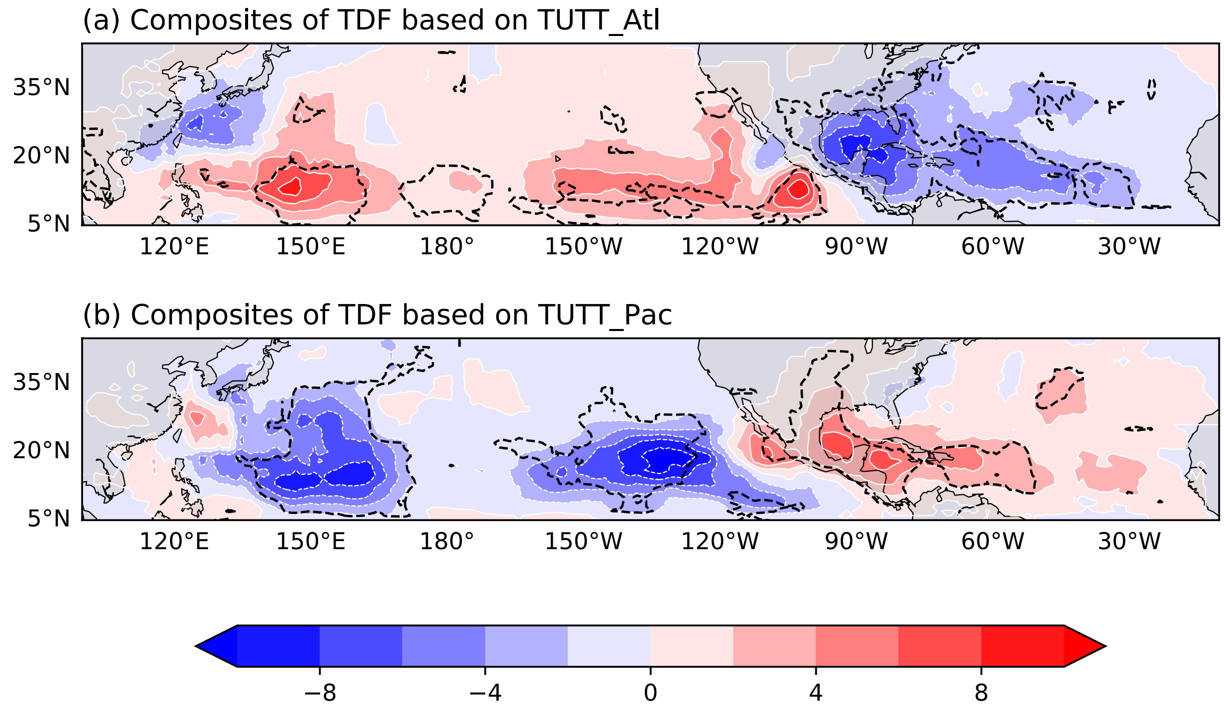

Figure 2 Composites of tropical cyclone track density function (units: number of TCs per month within a 10º×10º grid box) based on (a) TUTT_Atl and (b) TUTT_Pac. Dashed contours depict the anomalies exceeding the 95% confidence level.

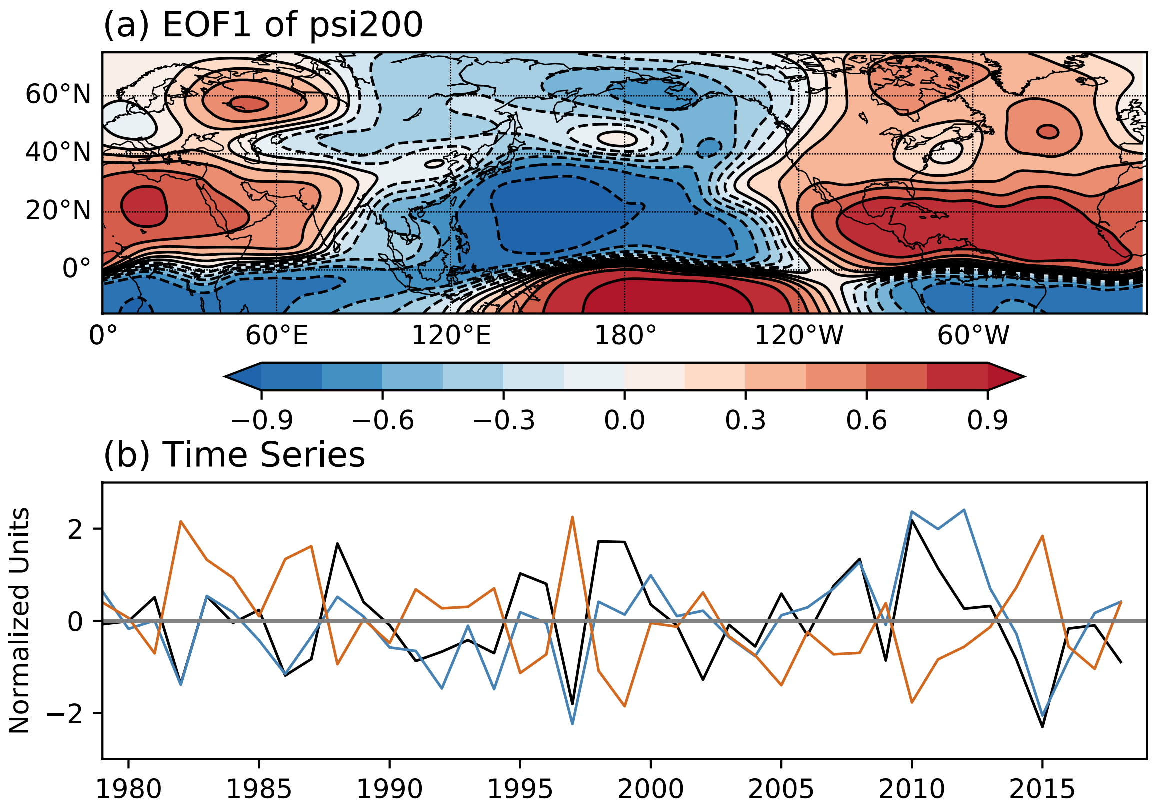

Figure 3 (a) The first EOF mode of 200-hPa streamfunction (scaled to unit variance); (b) the normalized time series of EOF1 (black), TUTT_Pac (blue), and TUTT_Atl (brown).

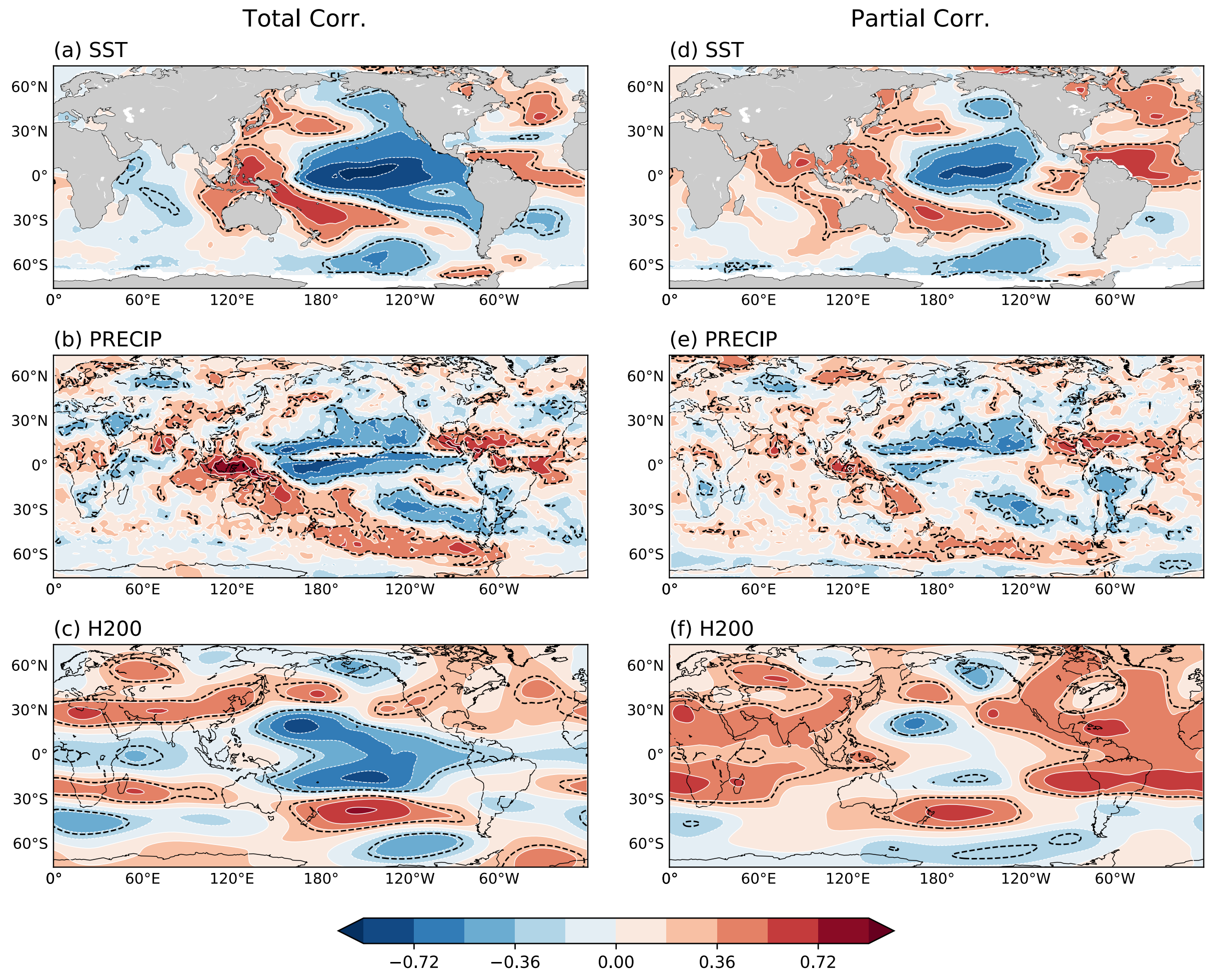

Figure 4 Correlations of the EOF1 time series with (top) SST, (middle) precipitation and (bottom) 200-hPa geopotential height. The total correlations are shown in the left column (a-c), and the right column (d-f) shows the partial correlations with the Nino3.4 index controlled. Dashed contours depict the correlation coefficients exceeding the 95% confidence level.

Table 1 Correlation coefficients between different climate indices and the TC activity indices over three basins during JASO 1979-2018. RWB is the RWB frequency between 10-85ºW, south of the jet axis and north of 20ºN (see Zhang et al. 2017 for more details). Most correlations exceed the 95% confidence level, and those below the 95% confidence level are highlighted by an asterisk.

	TCF	**HURR**	**ACE**
Corr.	**Atlantic TC Indices**		
TUTT_Atl	-0.73	-0.76	-0.75
MDR	0.59	0.56	0.55
Nino3.4	-0.34	-0.38	-0.32
RWB	-0.46	-0.56	-0.68
EOF1	0.54	0.58	0.50
	East Pacific TC Indices		
TUTT_Pac	-0.60	-0.58	-0.63
Nino3.4	0.39	0.28*	0.46
EOF1	-0.60	-0.50	-0.58
	West Pacific TC Indices		
TUTT_Pac	-0.45	-0.53	-0.61
Nino3.4	0.01*	0.18*	0.56
EOF1	-0.30*	-0.46	-0.69

Supplementary Information for

Summertime Stationary Waves Integrate Tropical and Extratropical Impacts on Tropical Cyclone Activity

Zhuo Wang, Gan Zhang, Timothy J. Dunkerton and Fei-Fei Jin

corresponding author: Zhuo Wang
Email: zhuowang@illinois.edu

This PDF file includes:

Figures S1 to S10
Tables S1 to S2

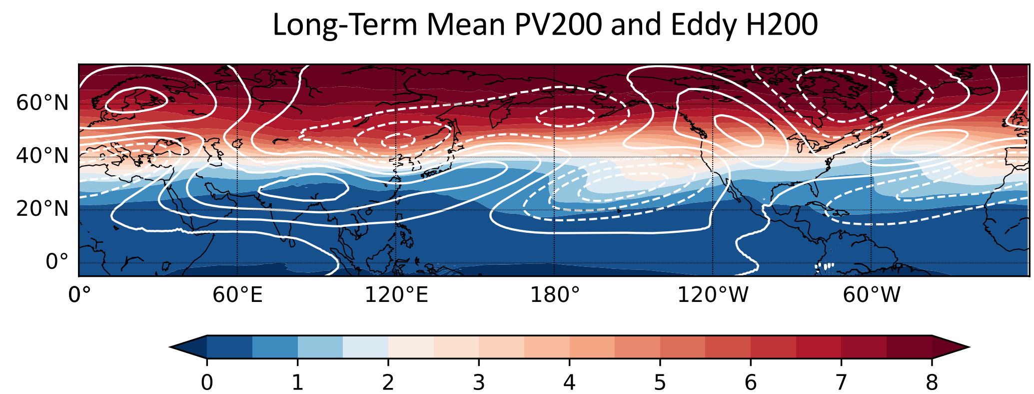

Fig. S1 Long-term mean (1979-2018) 200-hPa potential vorticity (shading: units: PVU) and 200-hPa geopotential height (contours with the interval of 250 m). The zonal mean component is removed from the geopotential height field.

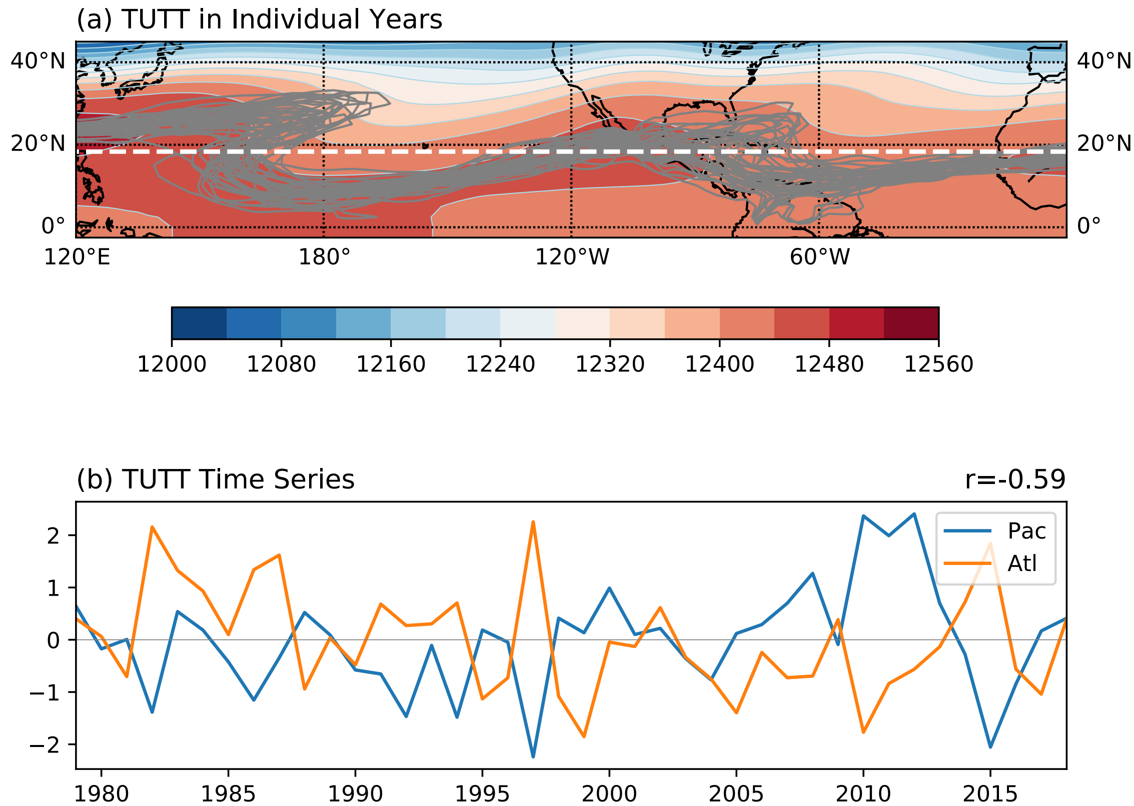

Fig. S2 (a) Long-term mean 200-hPa geopotential height (shading; units: m), the reference latitude for TUTTs (white dashed line; see text for details), and the contours of $u_g = 1.0\ m\ s^{-1}$ for individual years from 1979-2018; (b) the time series of the normalized TUTT_Pac and TUTT_Atl indices. The correlation between TUTT_Atl and TUTT_Pac is shown at the upper right corner of panel (b).

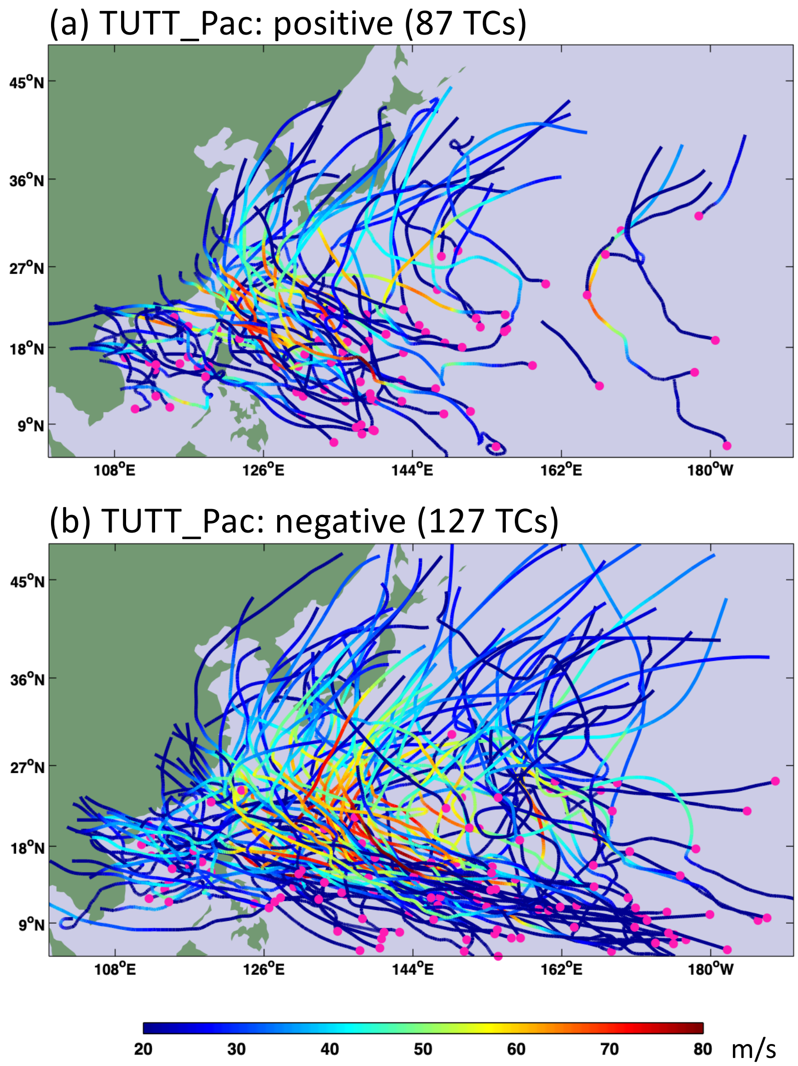

Fig. S3 Composites of TCs over the western North Pacific during (a) eight strong TUTT_Pac years and (b) eight weak TUTT_Pac years. Pink dots represent genesis locations, and colors along TC tracks indicate TC intensity in terms of the maximum surface wind speed. The numbers inside parentheses show the total number of TCs for each composite plot.

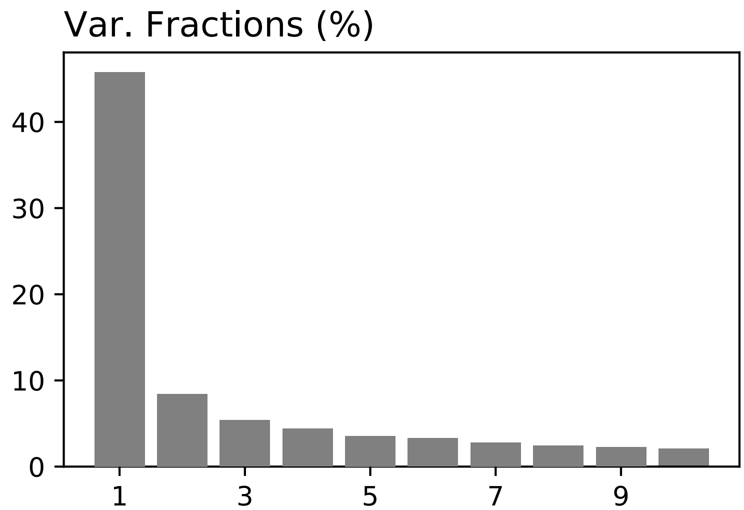

Fig. S4 The fractional contribution of the first ten EOF modes to the total variance.

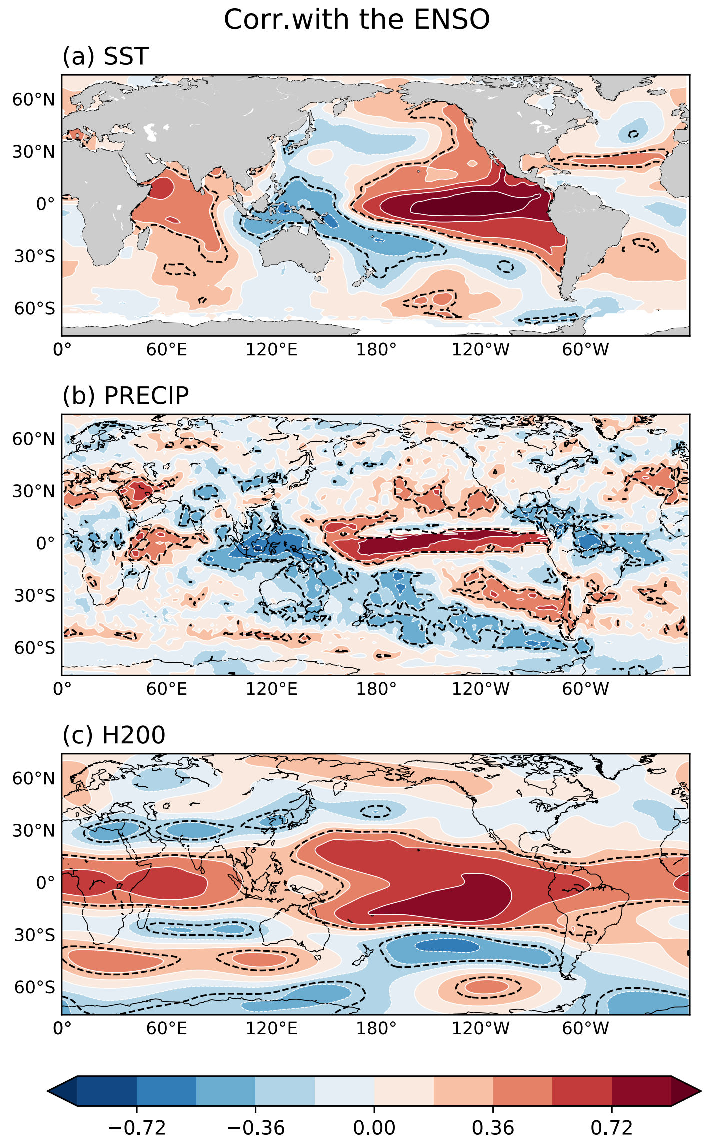

Fig. S5 Correlations of the Nino3.4 index with (a) SST, (b) precipitation, (c) H850 and (d) H200 during 1979-2018 JASO. Dashed contours depict the correlation coefficients exceeding the 95% confidence level.

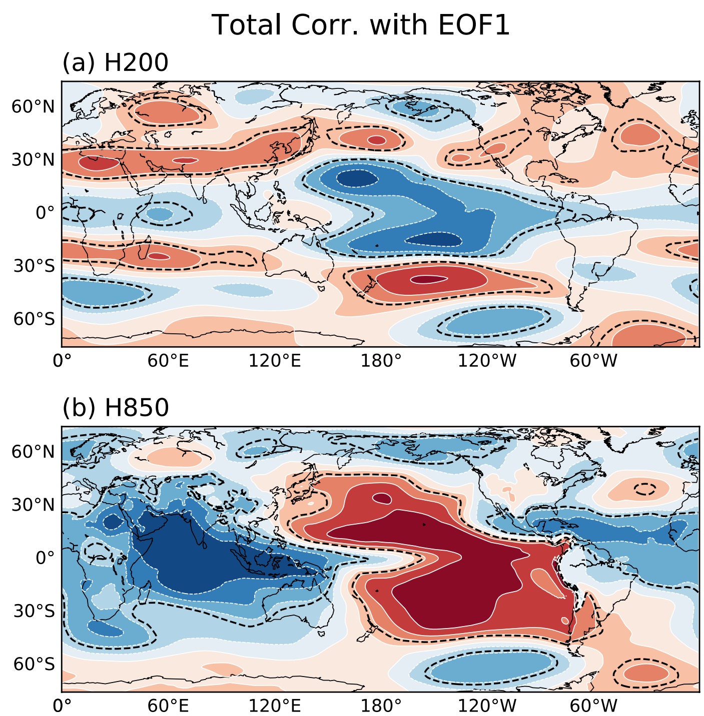

Fig. S6 Correlations of the EOF1 time series with (a) H200 and (b) H850. Dashed contours depict the correlation coefficients exceeding the 95% confidence level.

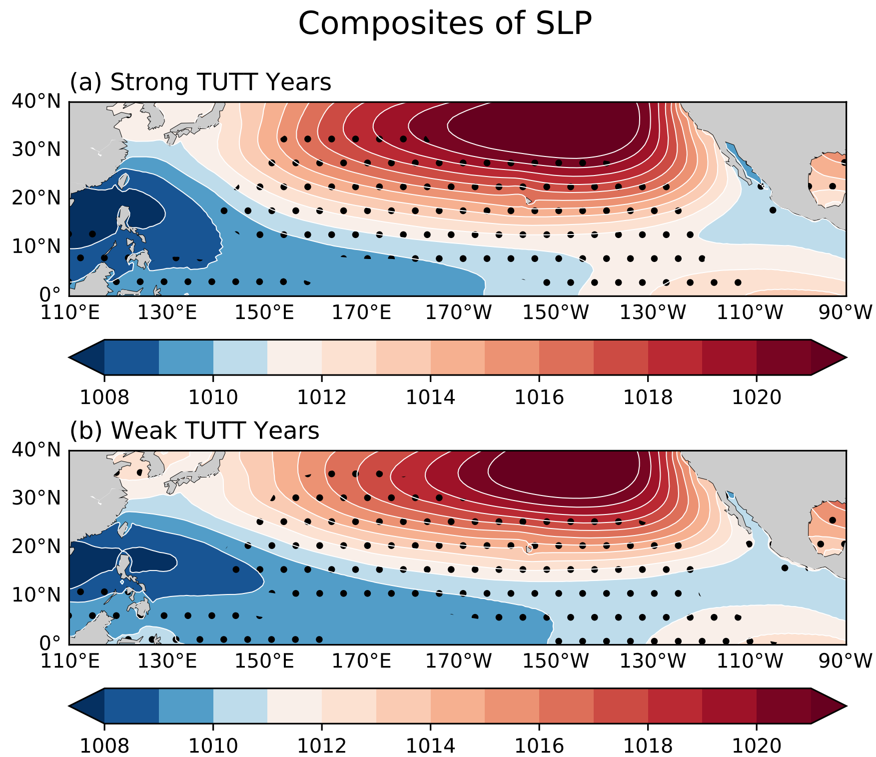

Fig. S7 Composite mean sea level pressure (SLP; hPa) for (a) strong and (b) weak TUTT_Pac years. Dots highlight where SLP differs significantly between the two phases.

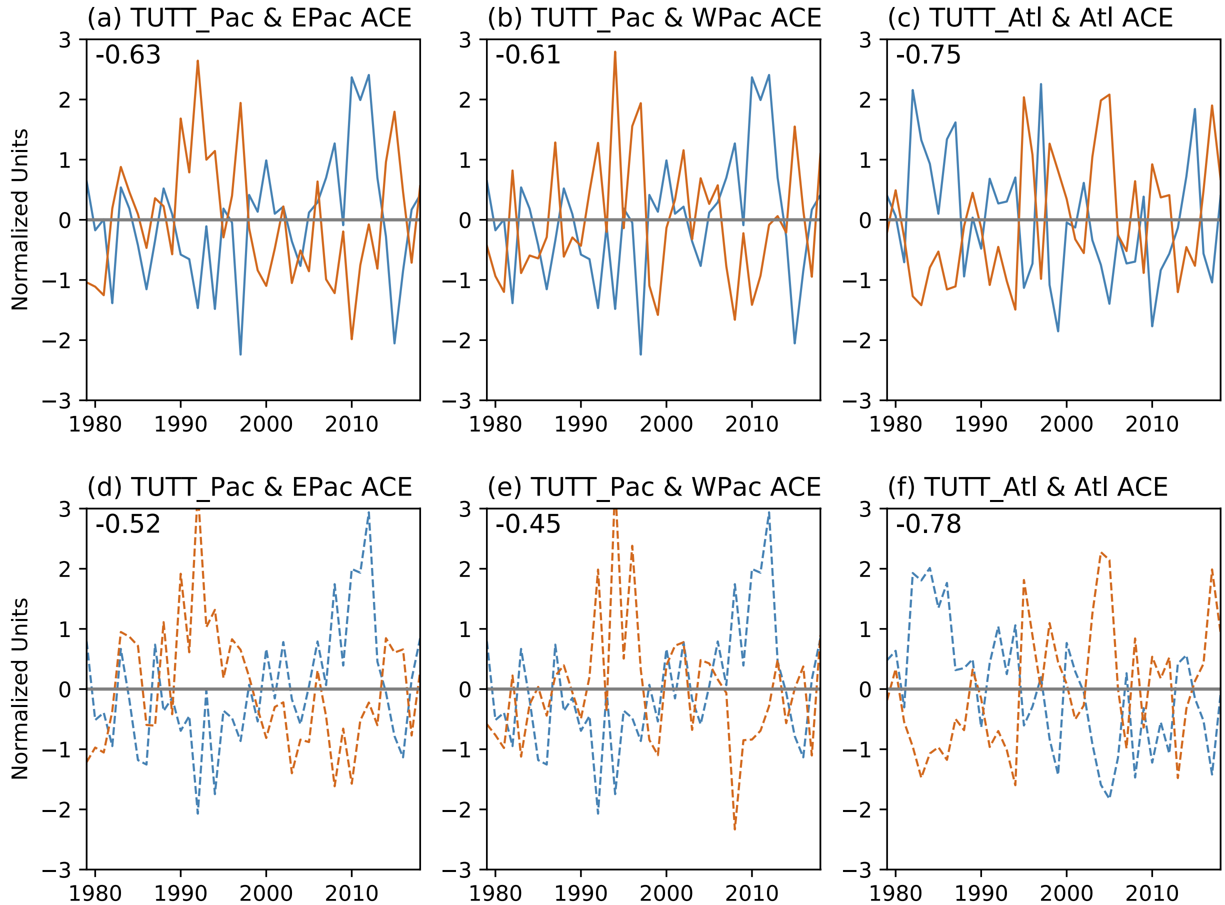

Fig. S8 (left) Time series of TUTT_Pac (blue) and the East Pacific ACE (brown); (middle) time series of TUTT_Pac (blue) and the West Pacific ACE (brown); and (right) time series of TUTT_atl (blue) and the North Atlantic ACE (brown). The top panels show the original data, and the bottom panels show the time series after the linear impacts of the ENSO are removed. The number at the upper left corner of a panel is the correlation between the illustrated time series. All the time series are normalized and shown for 1979-2018.

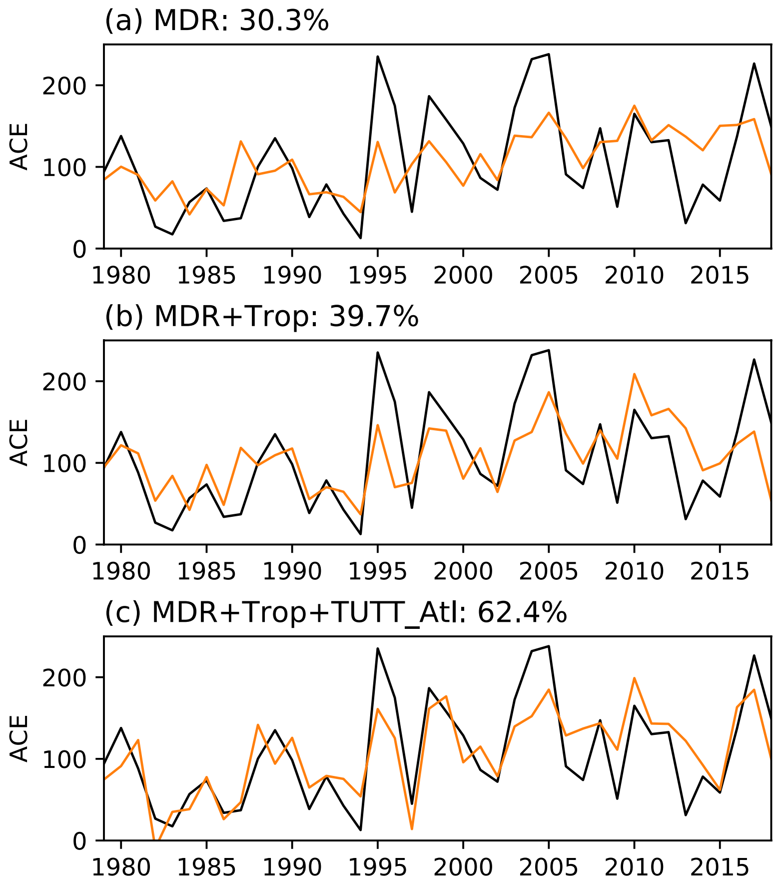

Fig. S9 The Atlantic ACE time series derived from IBTrACS (black) and reconstructed (orange) based on the linear regression of (a) MDR SST, (b) MDR SST and the tropical mean SST (Trop), and (c) MDR SST, tropical mean SST and TUTT_Atl. The numbers indicate the observed variance explained by the reconstructed ACE.

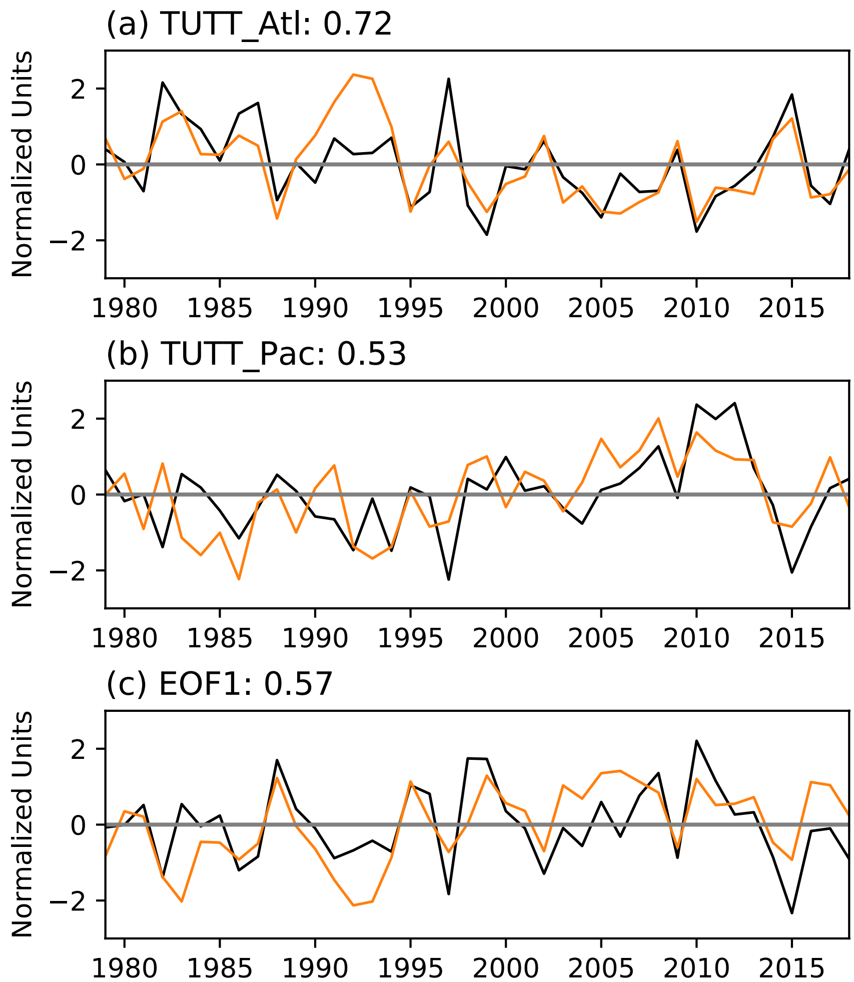

Fig. S10 Time series of the observed (black) and predicted (orange) time series of (a) TUTT_Atl, (b) TUTT_Pac, and (c) EOF1 (see the main text for more information). The numbers indicate the correlations between the predicted and observed time series.

Table S1 Composite years for the positive and negative phases of TUTT_Atl.

	TUTT_Atl	TUTT_Pac
Positive	1997, 1982, 2015, 1987, 1986, 1983, 1984, 2014	2012, 2010, 2011, 2008, 2000, 2013, 2007, 1979
Negative	1999, 2010, 2005, 1995, 1998, 2017, 1988, 2011	1997, 2015, 1994, 1992, 1982, 1986, 2016, 2004

Table S2 Correlations with various climate indices during JASO 1979-2018. Correlations below the 95% confidence level are highlighted by an asterisk.

	Nino3.4	PDO	PMM	MDR	AMM	AMO
EOF1	-0.79	-0.59	-0.26*	0.24*	0.50	0.25*
TUTT_Pac	-0.50	-0.65	-0.45	0.34	0.39	0.35
TUTT_Atl	0.71	0.62	-0.03*	-0.46	-0.65	-0.48